

# Right buffer sizing matters: stability and queuing dynamics in TCP

Debayani Ghosh, Krishna Jagannathan and Gaurav Raina

## Abstract

Motivated by recent concerns that queuing delays in the Internet are on the rise, we conduct a performance evaluation of Compound TCP (C-TCP) in two topologies: a single bottleneck and a multi-bottleneck topology. The first topology consists of a single core router, and the second consists of two distinct sets of TCP flows, regulated by two edge routers, feeding into a common core router. For both topologies, we develop fluid models and conduct a detailed local stability analysis in the small buffer regime, and obtain necessary and sufficient conditions for local stability. Further, we show that the underlying non-linear models undergo a Hopf bifurcation as the stability conditions just get violated. Using a combination of analysis and packet-level simulations, we emphasise that larger buffer thresholds, in addition to increasing latency, are prone to inducing limit cycles. These limit cycles in turn cause synchronisation among the TCP flows, and also result in a loss of link utilisation. For the single bottleneck topology, we empirically analyse some statistical properties of the bottleneck queue. We highlight that in a high bandwidth-delay product and a small buffer regime, and with a large number of long-lived flows, the bottleneck queue may be modelled as an  $M/M/1/B$  or an  $M/D/1/B$  queue. The combination of the dynamical and the statistical properties explored in this paper could have important implications for quality of service in the Internet.

## Index Terms

Compound TCP, Drop-Tail, Queue management, Local stability, Hopf bifurcation

## I. INTRODUCTION

There is an increasing concern regarding large queuing delays in today's Internet. This rise in queuing delays has primarily been attributed to a phenomenon called *bufferbloat*; *i.e.* the presence of large and persistently full buffers in Internet routers [3], [7]. Excessive queuing delays, caused by these large buffers, are a hindrance to the efficient functioning of congestion control algorithms implemented at end systems, thus adversely affecting the performance of the entire network.

End-to-end latency in the Internet is influenced by several factors, such as the size of router buffers, the flavour of TCP, and the choice of queue management scheme. Currently, three regimes for sizing router buffers have been

D. Ghosh, K. Jagannathan and G. Raina are with the Department of Electrical Engineering, IIT Madras, Chennai 600036, India. Email: {ee12s052, krishnaj, gaurav}@ee.iitm.ac.in

A part of this work appeared in [8].

proposed in the literature [20]: a large, an intermediate, and a small buffer regime. In practice, today’s router buffers are sized according to the traditional bandwidth-delay rule of thumb [25], which leads to larger buffers as bandwidth increases. While numerous flavours of TCP have been proposed in the literature, Compound TCP [24] is the default protocol in the Windows operating system and Cubic TCP [10] is used in Linux. As far as queue management is concerned, sophisticated solutions have been proposed in an attempt to eradicate the pervasive problem of excessively large buffers. The primary aim of an active queue management strategy is to keep the bottleneck queues small by probabilistically dropping or marking packets. Few examples of active queue management strategies are RED [5], CODEL [15], and PIE [17]. However, a simple Drop-Tail policy which just drops incoming packets if the router buffer is full, is widely deployed.

The bufferbloat phenomenon has been shown to be a concern in the context of wireless networks as well. In [22], the authors summarise the challenges associated with buffer sizing of routers in wireless networks, which are primarily due to the time-varying nature of the wireless channel capacity. In [13], the authors addressed the issue of bufferbloat in cellular networks, where large buffers are deployed at the base stations to smooth out bursty traffic. Further, the authors argue that rather than modifying the TCP at the sender side, or employing queue management strategies at the base station, it would be worthwhile to modify the TCP at the receiver side. To that end, the authors have proposed a simple receiver based solution, which could significantly reduce end-to-end latency and increase throughput in cellular networks.

Issues concerning large buffers and latency, continue to attract attention in the literature. For example, [27] explores the impact of reducing buffers in the presence of heterogeneous TCP flows. It is also being recognized that buffering dynamics can indeed play an important role in the stability of congestion controllers; see [23], and references therein. However, the models in [23] do not consider practically implemented protocols like Compound TCP or Cubic TCP as part of their study.

In this paper, our primary focus is on Compound TCP with a Drop-Tail queue policy and First-Come First-Serve (FCFS) service, in an intermediate and a small buffer regime. For completeness, we show that the models could also be used to analyse other flavours of TCP, such as Reno [16] and HighSpeed TCP [6]. Recent studies [26] have shown that 14.5%  $\sim$  25.66% of 30,000 web servers implement Compound TCP. Given the large fraction of web servers that currently use Compound TCP, analytical models for Compound have immense practical value.

Currently, there are very few analytically tractable models that have been proposed for Compound TCP in the literature. Recently, fluid models for a class of delay and loss-based protocols including Compound have been proposed [21]. In these models, the average window size of a large number of TCP flows is modelled using a non-linear, time-delayed dynamical system. This model has also been used to conduct a performance evaluation C-TCP in conjunction with the well-known Random Exponential Marking (REM) queue management policy [19].

The first topology we consider is a single bottleneck link, which either has a large number of long-lived flows, or a combination of long-lived and short-lived flows. For this topology, we focus on dynamical properties of the system, and some statistical properties of the bottleneck queue. We first conduct a local stability analysis, in the small buffer regime, and derive conditions that ensure local stability and non-oscillatory convergence. We then empirically

investigate the queue distribution when the buffer is small, and we have a large number of flows operating over a high bandwidth-delay regime. We find that the empirical queue distribution may be approximated rather well by either an  $M/M/1/B$  or an  $M/D/1/B$  queue. Thus, for the analysis, this allows us to use the drop probability of a small buffer Drop-Tail queue as the blocking probability of an  $M/M/1/B$  queue. For the empirical study, the packet-level simulations were conducted in NS2 [28].

The second topology consists of two distinct sets of long-lived flows, regulated by two separate edge routers, each having a different round trip time, and feeding into a common core router. For this topology, with heterogeneous network parameters and different round trip times, deriving the necessary and sufficient condition for local stability is analytically rather difficult. To make progress, we conduct the local stability analysis with two simplifying assumptions. In the first scenario, we assume that the router buffers and the bottleneck link capacities are the same, and the two sets of Compound TCP flows have the same average round trip times. In the second scenario, we assume the network parameters to be heterogeneous. However, the average round trip time of one set of TCP flows is taken to be much larger than the other. In addition, the round trip time of the second set of TCP flows is assumed to be negligible. It is worthwhile to mention that, for our local stability analysis, we approximate the drop probability at each router by the blocking probability of an  $M/M/1/B$  queue. The rationale behind this approximation is a direct consequence of the insight obtained from the statistical properties of the bottleneck queue in the single bottleneck topology.

In each of these topologies, a key insight obtained from our analysis is that smaller buffer thresholds are favourable for stability. Indeed, this insight holds even when short flows are present along with the long-lived flows. In addition, our analysis yields that, increasing buffer thresholds in the multiple bottleneck topology could prompt the system to lose stability, even if one of the round trip times is large. Smaller buffers would also lead to low latency, which is highly desirable.

Another important contribution of this paper lies in determining the behaviour of the system as it transits from a locally stable to a locally unstable regime. In particular, we prove that the dynamical system undergoes a Hopf bifurcation [9] when the conditions for local stability just get violated, in both the topologies. Two parameters play a very important role in ensuring stability: the feedback delay, and the size of the router buffer. For example, as the delay increases beyond a certain threshold, the system undergoes a Hopf bifurcation and loses local stability, when one pair of complex conjugate roots crosses over the imaginary axis. Since a Hopf bifurcation alerts us to the emergence of limit cycles, our analysis for both models, predicts the emergence of limit cycles when the necessary and sufficient conditions get violated. These limit cycles induce synchronisation of the TCP windows, and cause periodic oscillations in the queue occupancy. We confirm some of our analytical insights by conducting extensive packet-level simulations. Notably, the predictions of the fluid model agree remarkably well with the packet-level simulations even with a moderate number (about 60) of long-lived flows. The existence of limit cycles were repeatedly observed in the packet-level simulations. It is thus natural to have an analytical framework to establish the existence and determine the asymptotic orbital stability of these limit cycles. In a sequel to this work, we provide a detailed local bifurcation theoretic study of the various models considered in this paper.

To summarise, our primary contribution is in highlighting the interplay between buffer thresholds and stability in the presence of feedback delays. In particular, larger queue thresholds would increase queuing delay, in addition to inducing limit cycles in the queue size dynamics. Such limit cycles can lead to a drop in link utilisation, induce synchronisation among TCP flows, and make the downstream traffic bursty. Secondly, we find that even in the presence of short flows, limit cycles in the queue do not disappear. In other words, the ‘noise’ contributed by the short flows does not serve to desynchronise the limit cycles emerging due to the dynamics of the long flows. Lastly, we explicitly show via packet-level simulations that the fluid models are indeed valid when there are a large number of long-lived flows and the bandwidth-delay product is high.

The rest of this paper is organised as follows. In Section II, we briefly outline the congestion avoidance algorithm of Compound TCP. In Section III, we analyse a single bottleneck topology with long-lived, and a combination of long and short flows. Some of our analytical insights are corroborated by simulations, conducted at the packet-level, in the Network Simulator (NS2) [28]. In Section IV, we study a multi-bottleneck topology using a combination of analysis and packet-level simulations. Finally, in Section V we summarise our contributions.

## II. COMPOUND TCP

Compound TCP (C-TCP) [24] is a widely implemented Transmission Control Protocol (TCP) in the Windows operating system. Transport protocols like Reno and HighSpeed (HSTCP) use packet loss as the only indication of congestion, and protocols like Vegas [1] uses only queuing delay as the measure of network congestion. C-TCP is a synergy of both loss and delay-based feedback. The motivation behind incorporating both forms of feedback in C-TCP is to achieve high link utilisation and also to provide fairness to other competing TCP flows.

Compound TCP incorporates a scalable delay-based component into the congestion avoidance algorithm of TCP Reno. C-TCP controls its packet sending rate by maintaining two windows, a loss window  $cwnd$  and a delay window  $dwnd$ . In a time period of one round trip time, C-TCP updates its sending window  $w$  as follows:

$$w = \min(cwnd + dwnd, awnd). \quad (1)$$

Here,  $awnd$  is the advertised window at the receiver side. The decision function (1) governing the evolution of the sending window guarantees flow control between the source and the destination if the end systems operate at different speeds. In our paper, we assume that the sending window is constrained only by the congestion in the network path and not by the congestion at the receiver. Hence, for C-TCP, the source’s sending window will always be  $cwnd + dwnd$ . The loss window  $cwnd$ , behaves similar to the loss window of TCP Reno and follows the Additive Increase and Multiplicative Decrease (AIMD) rule whereas the delay window  $dwnd$ , controls the delay-based component. If there is no loss detected,  $cwnd$  increases by one packet in one round trip time and reduces by half whenever a loss is signalled. The algorithm for the delay-based component of Compound TCP is motivated from TCP Vegas. A state variable,  $baseRTT$  gives the transmission delay of a packet in the network path. If the current round trip time of the TCP flow is  $RTT$ , then

$$diff = \left( \frac{w}{baseRTT} - \frac{w}{RTT} \right) baseRTT,$$

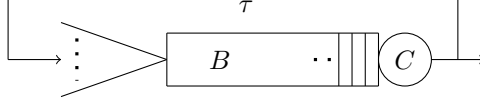


Fig. 1: Single bottleneck topology with multiple TCP flows feeding into a router. The bottleneck queue has buffer size  $B$  and link capacity  $C$ .

gives the amount of backlogged data in the bottleneck queue. If  $diff$  is less than the congestion threshold  $\gamma$ , the network is considered underutilised and the TCP flow increases its packet sending rate. If  $diff$  exceeds  $\gamma$ , congestion is detected in the network path which prompts the TCP flow to decrease its delay-based component. In C-TCP implementation, the default value of  $\gamma$  is fixed to be 30 packets. The overall behaviour of the window size of a C-TCP sender can then be summarised by combining the loss window and the delay window. When there is no congestion in the network path, neither in terms of increased queuing delay nor packet losses, a C-TCP sender increases its window size in its congestion avoidance phase as follows:

$$w(t+1) = w(t) + \alpha w(t)^k. \quad (2)$$

Here,  $\alpha$ ,  $k$  are the increase parameters and their default values are  $\alpha = 0.125$  and  $k = 0.75$  [24] respectively. If a packet loss is detected, the window size is multiplicatively reduced as follows:

$$w(t+1) = w(t)(1 - \beta). \quad (3)$$

Here,  $\beta$  is the decrease parameter and its default value is  $\beta = 0.5$  [24].

### III. SINGLE BOTTLENECK

This topology consists of a single bottleneck link with *many* TCP flows feeding into a core router employing a Drop-Tail queue policy, see Fig. 1. The flows are subject to a common round trip time  $\tau$ . Let the *average* window size of the flows be  $w(t)$ . Then the average rate at which packets are sent is approximately  $x(t) = w(t)/\tau$ . Let the average congestion window increase by  $i(w(t))$  for each received acknowledgement and decrease by  $d(w(t))$  for each packet loss detected. The following non-linear, time-delayed differential equation describes the evolution of the average window size in the congestion avoidance phase [21]

$$\frac{dw(t)}{dt} = \frac{w(t-\tau)}{\tau} \left( i(w(t)) (1 - p(t-\tau)) - d(w(t)) p(t-\tau) \right), \quad (4)$$

where  $p(t)$  denotes the loss probability experienced by packets sent at time  $t$ . We analyse (4) in two scenarios: one, in which all TCP flows are long-lived and another in which the traffic is a combination of both long and short flows. Since the loss probability  $p(t)$  depends on the window size  $w(t)$ , (4) now becomes

$$\dot{w}(t) = \frac{w(t-\tau)}{\tau} \left( i(w(t)) (1 - p(w(t-\tau))) - d(w(t)) p(w(t-\tau)) \right). \quad (5)$$

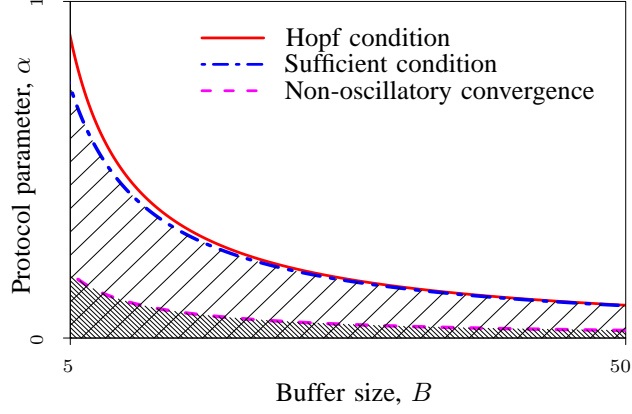


Fig. 2: *Stability Chart for single bottleneck topology.* Hopf condition, sufficient condition for local stability and condition for non-oscillatory convergence for compound TCP. The stability chart captures the intrinsic trade-off between the increase parameter  $\alpha$ , and buffer threshold  $B$ . Note that, as  $B$  increases,  $\alpha$  has to be reduced to ensure stability.

The equilibrium of system (5) satisfies

$$i(w^*)(1 - p(w^*)) = d(w^*)p(w^*). \quad (6)$$

Our focus will be on C-TCP, however other variants of TCP, like TCP Reno and HighSpeed TCP, can also be analysed via (5). The following are the functional forms of  $i(w(t))$  and  $d(w(t))$  for Compound, Reno and HighSpeed TCP.

- Compound TCP

$$i(w(t)) = \frac{\alpha (w(t))^k}{w(t)} \text{ and } d(w(t)) = \beta w(t). \quad (7)$$

- TCP Reno

$$i(w(t)) = \frac{1}{w(t)} \text{ and } d(w(t)) = \frac{w(t)}{2}. \quad (8)$$

- HighSpeed TCP

$$i(w(t)) = \frac{f_1(w(t))}{w(t)} \text{ and } d(w(t)) = f_2(w(t)) w(t), \quad (9)$$

where  $f_1(\cdot)$  and  $f_2(\cdot)$  are continuous functions of the window size. We now proceed to conduct a detailed local stability analysis for (5) to obtain sufficient, and necessary and sufficient conditions for local stability. We then particularise these conditions for Compound TCP, TCP Reno and HighSpeed TCP, and highlight the effects of buffer thresholds and protocol parameters on stability.

### A. Local stability and Hopf bifurcation analysis with long-lived flows

We let  $u(t) = w(t) - w^*$ , and linearise (5) about its non-trivial equilibrium point  $w^*$  to get

$$\dot{u}(t) = -au(t) - bu(t - \tau), \quad (10)$$

where

$$\begin{aligned} a &= -\frac{w^*}{\tau} (i'(w^*)(1 - p(w^*)) - d'(w^*)p(w^*)), \text{ and} \\ b &= \frac{w^*}{\tau} p'(w^*)d(w^*). \end{aligned} \quad (11)$$

Looking for exponential solutions of (10), we get

$$\lambda + a + be^{-\lambda\tau} = 0. \quad (12)$$

From [18], if  $a \geq 0$ ,  $b > 0$ ,  $b > a$  and  $\tau > 0$ , a sufficient condition for stability of (10) is

$$b\tau < \frac{\pi}{2}, \quad (13)$$

a necessary and sufficient condition for stability of (10) is

$$\tau\sqrt{b^2 - a^2} < \cos^{-1}(-a/b), \quad (14)$$

and the system undergoes the first Hopf bifurcation at

$$\tau\sqrt{b^2 - a^2} = \cos^{-1}(-a/b). \quad (15)$$

We now state conditions for local stability and Hopf bifurcation for Compound, Reno and HighSpeed TCP, with long-lived flows. We consider the case where the core router has small buffer size and deploy Drop-Tail queue policy. As argued in [20], for a large number of flows, the packet drop probability of a small buffer Drop-Tail queue can be approximated by the blocking probability of an  $M/M/1/B$  queue. Then, the drop probability of the bottleneck queue at equilibrium is [21]

$$p(w^*) = \left(\frac{w^*}{C\tau}\right)^B, \quad (16)$$

where  $C$  is the capacity of the bottleneck link,  $B$  is the buffer size and  $w^* = x^*\tau$ .

- *Compound TCP.* A necessary and sufficient condition for local stability with Compound TCP flows is [21]

$$\alpha(w^*)^{k-1} \sqrt{B^2 - ((k-2)(1 - p(w^*)))^2} < \cos^{-1} \left( \frac{(k-2)(1 - p(w^*))}{B} \right),$$

and a Hopf bifurcation would occur at

$$\alpha(w^*)^{k-1} \sqrt{B^2 - ((k-2)(1 - p(w^*)))^2} = \cos^{-1} \left( \frac{(k-2)(1 - p(w^*))}{B} \right).$$

- *TCP Reno*. Using the increase and decrease functions given by (8) and the fluid approximation of small buffer Drop-Tail queues given by (16), we get a necessary and sufficient condition for local stability as

$$\frac{1}{w^*} \sqrt{B^2 - 4(1 - p(w^*))^2} < \cos^{-1} \left( \frac{-2(1 - p(w^*))}{B} \right).$$

From (15), we note that a system with TCP Reno flows will undergo a Hopf bifurcation at

$$\frac{1}{w^*} \sqrt{B^2 - 4(1 - p(w^*))^2} = \cos^{-1} \left( \frac{-2(1 - p(w^*))}{B} \right). \quad (17)$$

- *HighSpeed TCP*. A necessary and sufficient condition for local stability for a system with High Speed TCP is

$$\begin{aligned} & \frac{f_1(w^*)}{w^*} \sqrt{B^2 - \left( \frac{w^* f_1'(w^*)}{f_1(w^*)} - 2 - \frac{(w^*)^3 f_2'(w^*) p(w^*)}{f_1(w^*)} \right)^2 (1 - p(w^*))^2} \\ & < \cos^{-1} \left( \frac{\left( \frac{w^* f_1'(w^*)}{f_1(w^*)} - 2 - \frac{(w^*)^3 f_2'(w^*) p(w^*)}{f_1(w^*)} \right) (1 - p(w^*))}{B} \right). \end{aligned}$$

Using condition (15), the associated Hopf condition can be stated. Clearly, the functional forms of  $i(w^*)$ ,  $d(w^*)$  and the model for the queue all greatly influence stability. Additionally, protocol parameters like  $\alpha$  and  $k$ , and network parameters like queue thresholds or buffer sizes have to be chosen rather carefully if stability is to be ensured.

### B. Non-oscillatory convergence with long-lived flows

Given these various conditions of stability, we now proceed to state a condition for non-oscillatory convergence of equation (10). For non-oscillatory convergence, we seek conditions on model parameters  $a$ ,  $b$  and the delay  $\tau$  for which the characteristic equation (12) has negative real solution.

*Theorem 1:* The solution of the system shows non-oscillatory convergence if and only if the parameters  $a$ ,  $b$  and  $\tau$  satisfy the condition  $\ln(b\tau) + a\tau + 1 < 0$ .

*Proof:* The boundary condition for the solution of (10) to be non-oscillatory is the point at which the curve  $f(\lambda) = \lambda + a + be^{-\lambda\tau}$  touches the real axis. If this point is  $\sigma$ , then

$$f(\sigma) = \sigma + a + be^{-\sigma\tau} = 0, \text{ and} \quad (18)$$

$$f'(\sigma) = 1 - b\tau e^{-\sigma\tau} = 0. \quad (19)$$

From (19), we get

$$be^{-\sigma\tau} = \frac{1}{\tau} \text{ and } \sigma = \frac{\ln(b\tau)}{\tau}. \quad (20)$$

Substituting values of  $\sigma$  and  $be^{-\sigma\tau}$  in (18) gives

$$\ln(b\tau) + a\tau + 1 = 0. \quad (21)$$

Then, a condition for non-oscillatory convergence of the equilibrium point is

$$\ln(b\tau) + a\tau + 1 < 0. \quad (22)$$



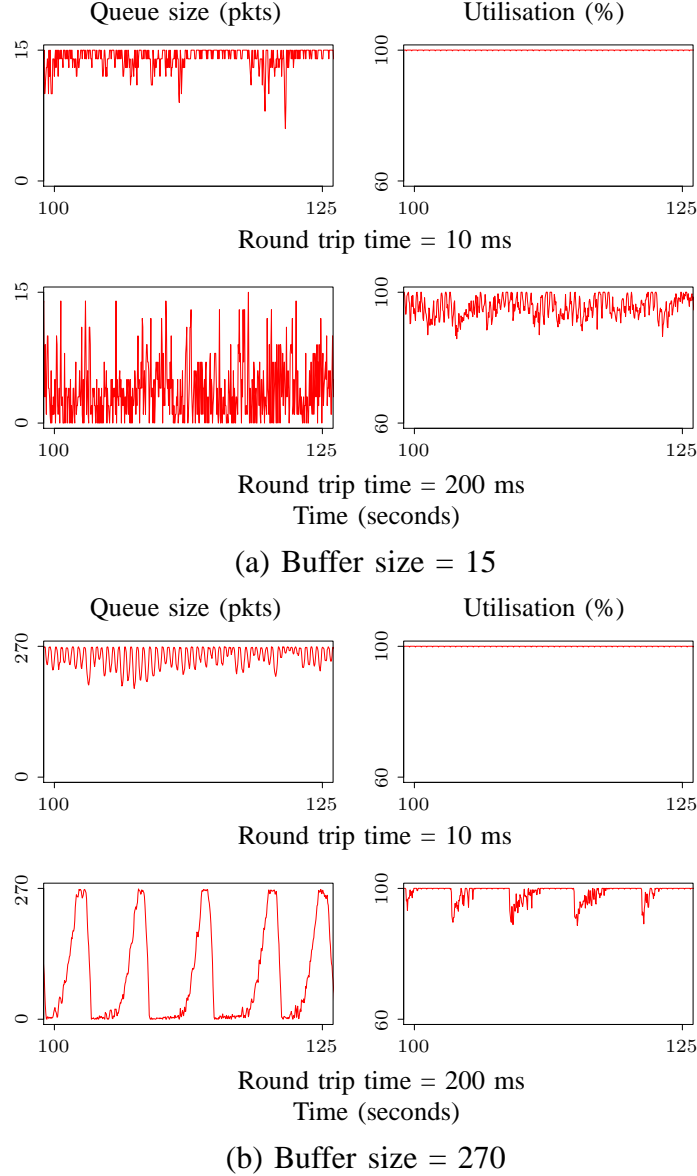


Fig. 3: *Long-lived flows*. 60 long-lived Compound TCP flows over a 2 Mbps link feeding into a single bottleneck queue with link capacity 100 Mbps.

- *Compound TCP*. The condition for non-oscillatory convergence with Compound TCP is

$$\alpha B (w^*)^{k-1} < \exp \left( \alpha (k-2) (w^*)^{k-1} (1 - p(w^*)) - 1 \right).$$

We can immediately observe the relation between the protocol parameters  $\alpha$  and  $k$ , and the network parameters like the buffer size  $B$  in ensuring that convergence of the equilibrium point is non-oscillatory.

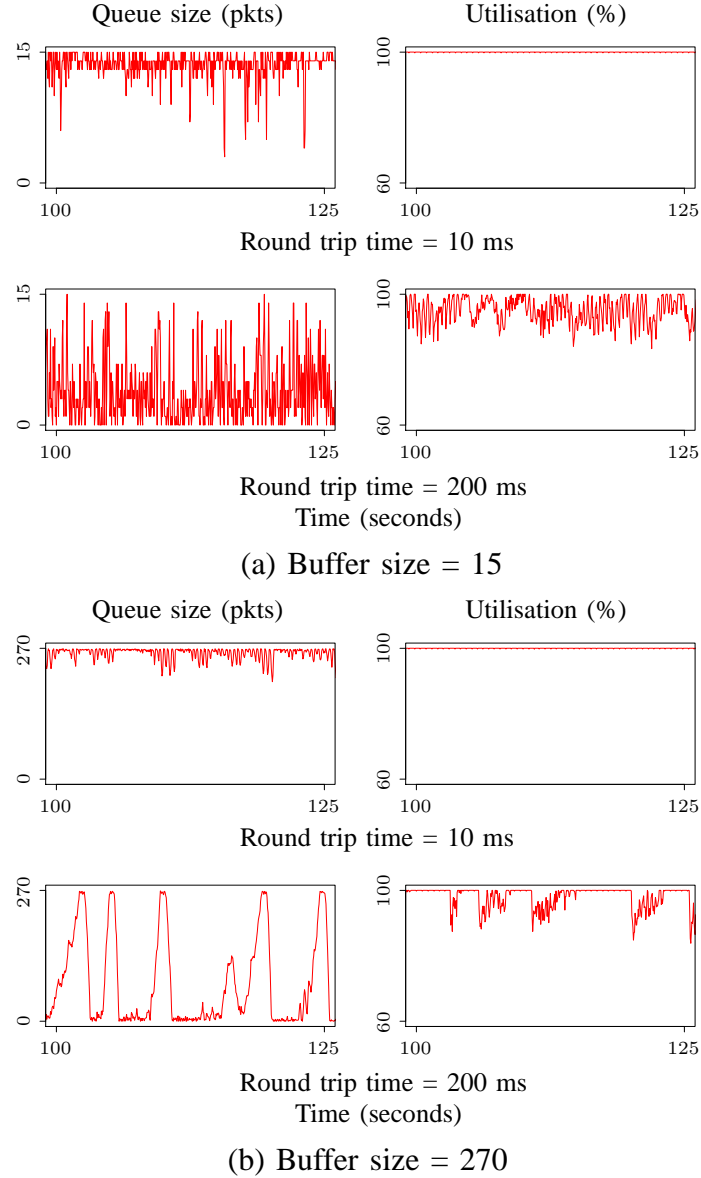


Fig. 4: *Long-lived and short-lived flows*. 60 long-lived Compound TCP flows over a 2 Mbps link, and *exponentially distributed short files*, feeding into a single bottleneck queue with link capacity 100 Mbps.

- *TCP Reno*. The condition for TCP Reno is

$$B < w^* \exp \left( -\frac{2}{w^*} (1 - p(w^*)) - 1 \right).$$

This condition highlights the central role played by the parameter  $B$  to ensure non-oscillatory convergence.

- *HighSpeed TCP*. With HSTCP flows, the corresponding condition is

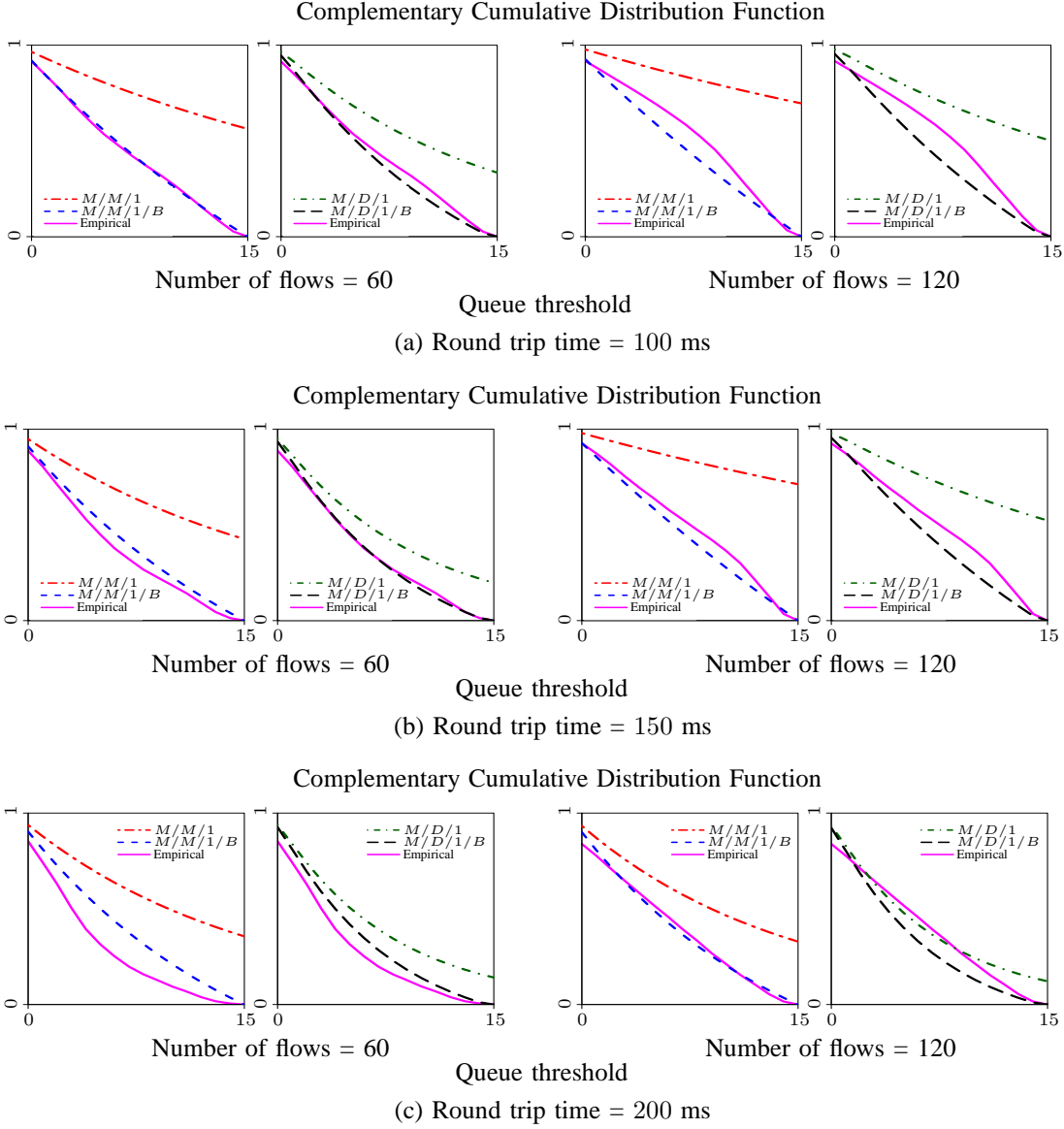


Fig. 5: *Statistics of the queue size.* Empirical queue length distribution for single bottleneck topology with 60 and 120 long-lived flows each having an access speed of 2 Mbps, and 1 Mbps respectively for round trip times (a) 100 ms, (b) 150 ms and (c) 200 ms. We compare the empirical queue statistics with the queue length distributions of  $M/M/1$ ,  $M/D/1$ ,  $M/M/1/B$ , and  $M/D/1/B$  for three different round trip times.

$$f_1(w^*)B < w^* \exp(A(w^*) - 1),$$

where,  $A(w^*) = \frac{f_1(w^*)}{w^*} \left( \frac{w^* f_1'(w^*)}{f_1(w^*)} - 2 - \frac{(w^*)^3 f_2'(w^*) p(w^*)}{f_1(w^*)} \right)$ . Clearly functional forms of  $f_1(w^*)$  and  $f_2(w^*)$ , and the choice of the parameter  $B$ , all have a role to play. It is thus clear that both design of transport protocols and queue management policies influence the dynamics of the system. To facilitate a better understanding of the analytical results derived above, we present a stability chart as shown in Fig. 2. Since, in this paper, we primarily

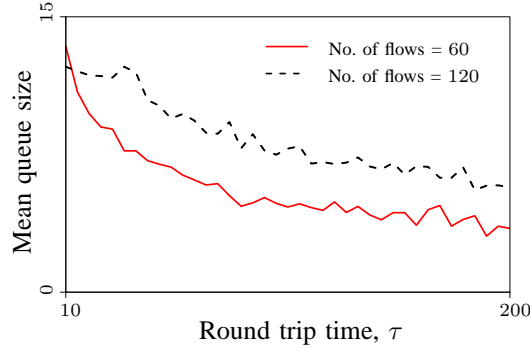


Fig. 6: *Mean queue size*. Evolution of mean queue size as a function of round trip time. We consider the number of long-lived flows to be 60 and 120 with link access speeds being 2 Mbps and 1 Mbps respectively.

focus on the performance of Compound TCP, we illustrate the stability chart in terms of its protocol parameter  $\alpha$  and buffer threshold  $B$ . This characterises the Hopf Condition, sufficient condition for local stability and condition for non-oscillatory convergence for Compound TCP with a large number of long-lived flows in the single bottleneck scenario. The stability chart complements our analytical insight in the sense that as buffer size is increased, the protocol parameter  $\alpha$  has to be decreased to ensure both stability and non-oscillatory convergence of the system.

### C. Local stability and Hopf bifurcation analysis with long-lived and short-lived flows

We now deviate from the assumption that the system has only long-lived flows and consider the scenario where the traffic consists of both long and short flows. On a short time scale, short TCP connections may act as an uncontrolled and random background load on the network. Suppose the workload arriving at the bottleneck queue over a time period  $T$  is modelled as Gaussian with mean  $x^*T$  and variance  $x^*\sigma_1^2T$  and the background load due to the short transfers over the time period  $T$  is also modelled as Gaussian with mean  $vT$  and variance  $v\sigma_2^2T$ . Then the loss probability at the bottleneck queue can be expressed as [14]

$$p(w^*) = \exp\left(\frac{-2B(C\tau - w^* - v\tau)}{w^*\sigma_1^2 + v\sigma_2^2\tau}\right). \quad (23)$$

Recall that (13) gives a sufficient condition for local stability and (15) gives the condition for which the system undergoes a Hopf-type bifurcation. We now particularise the sufficient condition for Compound TCP, TCP Reno and HighSpeed TCP. We are also in a position to state the Hopf bifurcation conditions, which are left out due to space constraints.

- *Compound TCP*. For Compound TCP, a sufficient condition for local stability of the system is

$$2B\alpha(w^*)^k \tau \frac{v\sigma_2^2 + (C - v)\sigma_1^2}{(w^*\sigma_1^2 + v\sigma_2^2\tau)^2} < \frac{\pi}{2}. \quad (24)$$

- *TCP Reno*. For TCP Reno, using the increase and decrease functions given by (8), we get a sufficient condition for stability as

$$2B\tau \frac{v\sigma_2^2 + (C-v)\sigma_1^2}{(w^*\sigma_1^2 + v\sigma_2^2\tau)^2} < \frac{\pi}{2}. \quad (25)$$

- *HighSpeed TCP*. With HSTCP flows, a sufficient condition for the local stability is

$$2Bf_1(w^*)\tau \frac{v\sigma_2^2 + (C-v)\sigma_1^2}{(w^*\sigma_1^2 + v\sigma_2^2\tau)^2} < \frac{\pi}{2}. \quad (26)$$

The conditions (24), (25) and (26) capture the relationships between the various protocol and network parameters. It is interesting to note that in general, larger the value of parameter  $B$ , greater the possibility of driving the system to an unstable state. In Compound TCP, there appears to be an intrinsic trade off in the choice of the parameter  $\alpha$  and the queue threshold parameter  $B$ . The presence of short-lived flows, which are modelled here as random uncontrolled traffic, does not change the requirement of choosing smaller values of  $B$  to ensure stability. We now present some packet-level simulations, which will enable us to comment on the dynamical and statistical properties of the system.

#### D. Simulations

*Dynamical Properties:* We now conduct packet-level simulations, using NS2 [28], for the single bottleneck topology in an intermediate and a small buffer sizing regime. With small buffers, we employ 15 packets. With intermediate buffers, the buffer dimensioning rule is  $B = C \cdot RTT / \sqrt{N}$ , where  $C$  is the bottleneck link capacity,  $RTT$  is the average round trip time of TCP flows and  $N$  is the number of long-lived flows in the system. Using this dimensioning rule, the bottleneck queue will have a buffer size of 270 packets. We consider two scenarios (i) only long-lived flows, and (ii) a combination of long and short flows. The bottleneck link has a capacity of 100 Mbps. The packet size is fixed at 1500 bytes. In either scenario, we consider 60 and 120 long-lived flows where each flow has an access link speed of 2 Mbps and 1 Mbps respectively. The file size of each of the short flows is exponentially distributed with a mean file size of 1 Mb. Since the dynamical properties of the underlying system for both 60 and 120 long-lived flows are qualitatively similar, we demonstrate simulations only for the case of 60 long-lived flows.

Fig. 3 depicts the simulations where the system only has long-lived flows. With small buffers, as expected, the queuing delay is negligible and the system is stable in the sense that there are no limit cycles in the queue size. With intermediate buffers, with smaller round trip times, the queues are full which yields full link utilisation but at the cost of extra latency. With larger delays, limit cycles will emerge in the queue size which also start to hurt link utilisation. Fig. 4 depicts the simulation results where the system has a combination of long and short-lived flows. Qualitatively, the results are very similar to those shown in Fig. 3. This is expected as the models did indeed predict that despite the presence of short flows the system could readily lose stability if key system parameters were not properly dimensioned.

*Statistical Properties:* First, in the small-buffer regime, *i.e.*, for buffer sizes of 15 and 100 packets, and small round trip times, the queue is almost full. Thus, the bottleneck queue acts as an integrator. Second, for a buffer size of 100 packets and larger round trip times, the queue dynamics exhibit stable limit cycles. Clearly, in these two cases, the queue size does not have a stationary distribution. Further, note that, for a buffer size of 15 packets and larger round trip times (200 ms), there are random fluctuations in the bottleneck queue. Hence, we focus on the statistical properties of the queue in the third regime.

In Fig. 5, we demonstrate the empirical complementary cumulative distribution of the queue size for a buffer size of 15 packets and 60 long-lived flows, each with an access speed of 2 Mbps, and with 120 long-lived flows each with an access speed of 1 Mbps. The round trip times which we consider are 100 ms, 150 ms and 200 ms. For each of these cases, we perform a comparative study of the empirical queue length distribution with the theoretical queue distributions of  $M/M/1$ ,  $M/D/1$ ,  $M/M/1/B$  and  $M/D/1/B$  queues. From the simulations we can infer that, with 60 long-lived flows, the empirical queue distribution can be reasonably approximated by the corresponding queue distribution of either an  $M/M/1/B$  or an  $M/D/1/B$  queue when the round trip time is large (100 ms). Notably, as the number of flows is increased to 120, this approximation holds true for larger round trip times perhaps due to increased statistical multiplexing. Indeed, it can be verified that, as the number of long-lived flows is increased further, this approximation holds true for even larger round trip time values. This serves to validate the packet drop probability at the core router and the fluid model in the regime with a large number of long-lived flows and high bandwidth-delay product. Fig. 6 illustrates the evolution of mean queue size as a function of round trip time for two scenarios. The first scenario consists of 60 long-lived Compound TCP flows, each with an access speed of 2 Mbps, while the second consists of 120 long-lived flows, each with an access speed of 1 Mbps. It can be immediately observed that, the mean queue sizes in the second scenario are larger than in the first scenario, for all round trip times. Due to increased statistical multiplexing, the average packet loss incurred by each user in the second scenario is less as compared to the first scenario. Consequently, the average arrival rate of packets at the bottleneck queue is larger in the second scenario. This is intuitive, since each TCP sender backs off less aggressively, owing to low packet loss. This, in turn, results in higher mean queue size in the second scenario, for all round trip times.

In the next section, we consider a multiple bottleneck topology which depicts a more realistic network scenario as opposed to the simple single bottleneck topology. For this topology, we will again consider the impact of long-lived, and a combination of long and short flows.

#### IV. MULTIPLE BOTTLENECKS

The model consists of two distinct sets of TCP flows having different round trip times  $\tau_1$  and  $\tau_2$  and regulated by two edge routers, as shown in Fig. 7. For this model, our focus will be on long-lived flows. The average window sizes of the two sets of flows are  $w_1(t)$  and  $w_2(t)$  respectively. The outgoing flows from both edge routers feed into a common core router. The buffer sizes of the edge routers are  $B_1$  and  $B_2$  respectively, and buffer size of the core router is  $B$ . The link capacities of the edge routers are  $C_1$  and  $C_2$  respectively. We consider the case

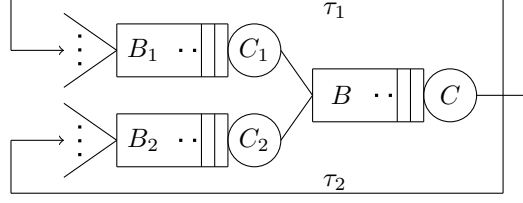


Fig. 7: Multiple bottleneck topology with two distinct sets of TCP flows, regulated by two edge routers, having round trip times  $\tau_1$  and  $\tau_2$  and feeding into a core router.

where both edge routers and the core router have small buffer sizes and employ a Drop-Tail queue policy. The link capacity of the core router is  $C$ . Suppose  $p_1(t)$  and  $p_2(t)$  are the packet loss probabilities at the two edge routers for the packets sent at time instant  $t$ , for the two distinct sets of flows respectively. The packet loss probability at the core router is denoted as  $q(t, \tau_1, \tau_2)$ . For a generalised TCP flavour, the non-linear, time-delayed, fluid model of the system is given by the following equations:

$$\dot{w}_j(t) = \frac{w_j(t - \tau_j)}{\tau_j} \left( i(w_j(t)) \left( 1 - p_j(t - \tau_j) - q(t, \tau_1, \tau_2) \right) - d(w_j(t)) \left( p_j(t - \tau_j) + q(t, \tau_1, \tau_2) \right) \right), j = 1, 2. \quad (27)$$

The loss probabilities at the three routers are approximated as

$$p_1(t) = \left( \frac{w_1(t)}{C_1 \tau_1} \right)^{B_1}, \quad p_2(t) = \left( \frac{w_2(t)}{C_2 \tau_2} \right)^{B_2}, \quad \text{and} \\ q(t, \tau_1, \tau_2) = \left( \frac{w_1(t - \tau_1)/\tau_1 + w_2(t - \tau_2)/\tau_2}{C} \right)^B.$$

In this section, we prove that even in the multiple bottleneck topology, the system loses stability through a *Hopf bifurcation* [9] as system parameters vary. This loss of local stability leads to the emergence of limit cycles in the queue size of the core router.

#### A. Necessary and sufficient condition for stability

For system (27), we will perform a local stability analysis to derive a necessary and sufficient condition for stability. Suppose the equilibrium of the system is  $(w_1^*, w_2^*)$ . Let  $u_1(t) = w_1(t) - w_1^*$  and  $u_2(t) = w_2(t) - w_2^*$  be small perturbations about  $w_1^*$  and  $w_2^*$  respectively. Linearising system (27) about its equilibrium  $(w_1^*, w_2^*)$ , we get

$$\begin{aligned} \dot{u}_1(t) &= -\mathcal{M}_1 u_1(t) - \mathcal{N}_1 u_1(t - \tau_1) - \mathcal{P}_1 u_2(t - \tau_2), \\ \dot{u}_2(t) &= -\mathcal{M}_2 u_2(t) - \mathcal{N}_2 u_2(t - \tau_2) - \mathcal{P}_2 u_1(t - \tau_1), \end{aligned} \quad (28)$$

where, for Compound TCP, the increase and decrease functions (7) yield the following coefficients

$$\begin{aligned}\mathcal{M}_j &= -\frac{\alpha}{\tau_j} (k-2) (w_j^*)^{k-1} \left( 1 - \left( \frac{w_j^*}{C_j \tau_j} \right)^{B_j} - \frac{1}{C^B} \left( \frac{w_1^*}{\tau_1} + \frac{w_2^*}{\tau_2} \right)^B \right), \\ \mathcal{N}_j &= \left( \alpha (w_j^*)^{k-1} + \beta w_j^* \right) \left( \frac{B_j}{\tau_j} \left( \frac{w_j^*}{C_j \tau_j} \right)^{B_j} + \frac{B (w_j^*)^2}{C^B \tau_j^2} \left( \frac{w_1^*}{\tau_1} + \frac{w_2^*}{\tau_2} \right)^{B-1} \right), \\ \mathcal{P}_j &= \left( \alpha (w_j^*)^{k-1} + \beta w_j^* \right) \frac{B w_j^*}{\tau_1 \tau_2 (C)^B} \left( \frac{w_1^*}{\tau_1} + \frac{w_2^*}{\tau_2} \right)^{B-1}, \quad j = 1, 2.\end{aligned}\tag{29}$$

At equilibrium, the following equations are satisfied

$$\alpha (w_j^*)^{k-1} \left( 1 - \left( \frac{w_j^*}{\tau_j C_j} \right)^{B_j} + \frac{1}{C^B} \left( \frac{w_1^*}{\tau_1} + \frac{w_2^*}{\tau_2} \right)^B \right) = \beta w_j^* \left( \frac{w_j^*}{\tau_j C_j} \right)^{B_j} + \frac{1}{C^B} \left( \frac{w_1^*}{\tau_1} + \frac{w_2^*}{\tau_2} \right)^B, \quad j = 1, 2.$$

For analytical tractability, we consider two different scenarios with simple assumptions. It is worthwhile to note that both scenarios are valid in the context of a real network.

#### Case I

In this scenario, we assume that the network parameters for all routers are the same *i.e.*  $B_1 = B_2 = B, C_1 = C_2 = C$ . We further assume that the round trip times of both sets of TCP flows are identical *i.e.*  $\tau_1 = \tau_2 = \tau$ . Then,  $w_1^* = w_2^* = w^*$  will be an equilibrium of the system, and satisfies the following equation:

$$\alpha (w^*)^{k-2} = \left( \alpha (w^*)^{k-2} + \beta \right) (1 + 2^B) \left( \frac{w^*}{\tau C} \right)^B.$$

Let  $\mathcal{M} = \frac{(\alpha (w^*)^{k-2} + \beta) B (w^*)^{B+1}}{\tau^{B+1} C^B}$ , then the coefficients  $\mathcal{M}_1, \mathcal{M}_2, \mathcal{N}_1, \mathcal{N}_2, \mathcal{P}_1, \mathcal{P}_2$  reduce to

$$\begin{aligned}\mathcal{M}_1 &= \mathcal{M}_2 = \frac{\mathcal{M} \beta w^*}{\left( \alpha (w_j^*)^{k-1} + \beta w_j^* \right)^B} (1 + 2^B) (2 - k) = a, \\ \mathcal{N}_1 &= \mathcal{N}_2 = \mathcal{M} (1 + 2^{B-1}) = b, \\ \mathcal{P}_1 &= \mathcal{P}_2 = \mathcal{M} 2^{B-1} = c.\end{aligned}\tag{30}$$

Note that  $a, b, c > 0$ . With these assumptions the linearised system (28) becomes

$$\begin{aligned}\dot{u}_1(t) &= -a u_1(t) - b u_1(t - \tau) - c u_2(t - \tau), \\ \dot{u}_2(t) &= -a u_2(t) - b u_2(t - \tau) - c u_1(t - \tau).\end{aligned}\tag{31}$$

**Theorem 2:** System (31) is stable if and only if the parameters  $a, b, c$  and  $\tau$  satisfy the condition  $\tau < \frac{1}{\omega_1} \cos^{-1} \left( \frac{-a}{b+c} \right)$  with crossover frequency  $\omega_1 = \sqrt{(b+c)^2 - a^2}$ .

*Proof:* Looking for exponential solutions, we get the characteristic equation for the linearised system (31) as

$$(\lambda + a + b e^{-\lambda \tau})^2 - c^2 e^{-2\lambda \tau} = 0,\tag{32}$$

which can be written as

$$g_1(\lambda) g_2(\lambda) = 0,$$



where,

$$\begin{aligned} g_1(\lambda) &= \lambda + a + (b + c)e^{-\lambda\tau}, \text{ and} \\ g_2(\lambda) &= \lambda + a + (b - c)e^{-\lambda\tau}. \end{aligned} \quad (33)$$

For stability, all roots of (32) should have negative real parts. For negligible values of delay  $\tau$ , system (31) is stable, *i.e.* all roots of the characteristic equation lie of the left half of the complex plane. As the delay is increased, the system becomes unstable if one pair of complex conjugate roots of either  $g_1(\lambda)$  or  $g_2(\lambda)$  or both crosses over the imaginary axis. We aim to determine the values of delay  $\tau$  at which one pair of complex conjugate roots of  $g_1(\lambda)$  and  $g_2(\lambda)$  cross over the imaginary axis. Let  $\tau_{1,c}$  and  $\tau_{2,c}$  denote the values of  $\tau$  at which  $g_1(\lambda)$  and  $g_2(\lambda)$  have exactly one pair of purely imaginary roots. Then, the critical value of  $\tau$ , denoted by  $\tau_c$ , at which (32) has one pair of purely imaginary roots is  $\tau_c = \min(\tau_{1,c}, \tau_{2,c})$  [2]. Substituting  $\lambda = j\omega_1$  in  $g_1(\lambda)$  and separating real and imaginary parts we get

$$(b + c) \sin \omega_1 \tau = \omega_1, \text{ and} \quad (34)$$

$$(b + c) \cos \omega_1 \tau = -a. \quad (35)$$

Solving (34) and (35) for  $\omega_1$  we get

$$\omega_1 = \sqrt{(b + c)^2 - a^2},$$

and under the condition  $b + c > a$ ,  $\omega_1^2$  is strictly positive. This implies that there exists a cross over frequency  $\omega_1$  at which one pair of complex conjugate roots of  $g_1(\lambda)$  crosses over to the right half of the complex plane. Solving (34) and (35) for  $\tau$ , we get the critical value of delay at which the system transits from stability to instability as

$$\tau_{1,c} = \frac{1}{\omega_1} \cos^{-1} \left( \frac{-a}{b + c} \right). \quad (36)$$

Similarly, substituting  $\lambda = j\omega_2$  in  $g_2(\lambda)$  we get the cross over frequency as

$$\omega_2 = \sqrt{(b - c)^2 - a^2}. \quad (37)$$

We substitute the coefficients  $a, b$  and  $c$  in (37) to get

$$\omega_2 = \mathcal{M} \sqrt{1 - \left( \frac{\beta(1 + 2^B)(k - 2)}{(\alpha(w^*)^{k-2} + \beta)B} \right)^2}. \quad (38)$$

It can be shown that,  $\omega_2$  does not exist for any integer value of the buffer size  $B$ , and default values of the protocol parameters. Hence, the roots of the characteristic equation  $g_2(\lambda)$  have negative real parts for all values of the delay  $\tau$ , implying that  $\tau_c = \tau_{1,c}$ . Consequently, all roots of the characteristic equation (32) lie on the left half of the complex plane for all  $\tau < \tau_c$ . Hence, system (31) is asymptotically stable for  $\tau < \tau_c$ , and unstable for  $\tau > \tau_c$ . Further, it can be analytically shown that this loss of stability occurs via a Hopf bifurcation when one pair of

complex conjugate roots of (32) crosses over the imaginary axis with non-zero velocity at  $\tau = \tau_c$ . Therefore, the necessary and sufficient condition for local stability of (31) is

$$\tau < \frac{1}{\omega_1} \cos^{-1} \left( \frac{-a}{b+c} \right). \quad (39)$$

■

Substituting values of  $\omega_1$ ,  $a$ ,  $b$  and  $c$  in (39), we get the necessary and sufficient condition for local stability of (27), with Compound TCP as

$$\alpha (w^*)^{k-1} \sqrt{B^2 - (k-2)^2 (1 - (1+2^B) p(w^*))^2} < \cos^{-1} \left( \frac{(k-2) (1 - (1+2^B) p(w^*))}{B} \right), \quad (40)$$

where  $p(w^*) = \left( \frac{w^*}{C\tau} \right)^B$ . This condition captures the relationship between the equilibrium window size, protocol parameters  $k$  and  $\alpha$ , and buffer size  $B$  of the core router to ensure stability of the system. If we increase the buffer size of the core router, keeping other parameters fixed, condition (40) would get violated.

### Case II

In this scenario, we assume that the network parameters for all routers are distinct, and the average round trip time of the first set of TCP flows is much larger than the other. Further, we consider that the average round trip time of the second set of TCP flows is negligible. This implies that  $\tau_1 \gg \tau_2$  and  $\tau_2 \approx 0$ . As a consequence of this assumption, the dynamics of the second set of TCP flows will appear to be almost instantaneous. This leads to the following non-linear, time-delayed fluid model of the system:

$$\begin{aligned} \dot{w}_1(t) &= \frac{w_1(t-\tau_1)}{\tau_1} \left( i(w_1(t)) \left( 1 - p_1(t-\tau_1) - q(t, \tau_1, \tau_2) \right) - d((w_1(t)) \left( p_1(t-\tau_1) + q(t, \tau_1, \tau_2) \right) \right), \\ \dot{w}_2(t) &= \frac{w_2(t)}{\tau_2} \left( i(w_2(t)) \left( 1 - p_2(t) - q(t, \tau_1, \tau_2) \right) - d((w_2(t)) \left( p_2(t) + q(t, \tau_1, \tau_2) \right) \right). \end{aligned} \quad (41)$$

The loss probabilities at the three routers are approximated as

$$\begin{aligned} p_1(t) &= \left( \frac{w_1(t)}{C_1 \tau_1} \right)^{B_1}, \quad p_2(t) = \left( \frac{w_2(t)}{C_2 \tau_2} \right)^{B_2}, \text{ and} \\ q(t, \tau_1, \tau_2) &= \left( \frac{w_1(t-\tau_1)/\tau_1 + w_2(t)/\tau_2}{C} \right)^B. \end{aligned}$$

We now proceed to perform a local stability analysis for system (41). This will enable us to characterise the stability of the system in the presence of heterogeneity in network parameters. Suppose  $(w_1^*, w_2^*)$  be a non-trivial equilibrium of system (41). Let  $u_1(t) = w_1(t) - w_1^*$  and  $u_2(t) = w_2(t) - w_2^*$  represent small perturbations about  $w_1^*$  and  $w_2^*$  respectively. Linearising system (41) about its equilibrium, we get the following:

$$\begin{aligned} \dot{u}_1(t) &= -\mathcal{M}_1 u_1(t) - \mathcal{N}_1 u_1(t-\tau_1) - \mathcal{P}_1 u_2(t), \\ \dot{u}_2(t) &= -(\mathcal{M}_2 + \mathcal{N}_2) u_2(t) - \mathcal{P}_2 u_1(t-\tau_1), \end{aligned} \quad (42)$$

where, the coefficients are given by (29). Looking for exponential solutions, we get the characteristic equation for the linearised system (42) as

$$\lambda^2 + a\lambda + b\lambda e^{-\lambda\tau_1} + ce^{-\lambda\tau_1} + d = 0, \quad (43)$$

where,

$$\begin{aligned} a &= \mathcal{M}_1 + \mathcal{M}_2 + \mathcal{N}_2, \quad b = \mathcal{N}_2, \\ c &= \mathcal{M}_1 (\mathcal{M}_2 + \mathcal{N}_2), \quad d = \mathcal{N}_1 (\mathcal{M}_2 + \mathcal{N}_2) - \mathcal{P}_1 \mathcal{P}_2. \end{aligned} \quad (44)$$

*Theorem 3:* System (42), having the characteristic equation (43) is stable if and only if the parameters satisfy the condition  $\tau_1 < \frac{1}{\omega} \cos^{-1} \left( \frac{\omega^2(d-ab)-cd}{b^2\omega^2+d} \right)$  with the cross over frequency as

$$\omega = \sqrt{\frac{(2c - a^2 + b^2)}{2} + \frac{\sqrt{(2c - a^2 + b^2)^2 - 4(c^2 - d^2)}}{2}}.$$

*Proof:* For system (42) to be stable, and hence system (41) to be locally stable about its equilibrium, all roots of the characteristic equation should lie on the left half of the complex plane. For negligible delays, system (42) can be shown to be stable. As  $\tau_1$  increases beyond a critical value, the system will transit into the unstable region if one pair of complex conjugate roots crosses over the imaginary axis. Following a similar kind of analysis as done in Case I, we can conclude that the system has a pair of purely imaginary complex conjugate roots with cross over frequency satisfying

$$\omega^2 = \frac{(2c - a^2 + b^2)}{2} \pm \frac{\sqrt{(2c - a^2 + b^2)^2 - 4(c^2 - d^2)}}{2}.$$

*Condition 1:* There exists only one positive value of  $\omega^2$  if the following conditions hold

- (i)  $(2c - a^2 + b^2) > 0$ , and  $(2c - a^2 + b^2)^2 = 4(c^2 - d^2)$ .
- (ii)  $(2c - a^2 + b^2) > 0$ , and  $c^2 - d^2 < 0$ .

*Condition 2:* There exists two positive value of  $\omega^2$  if the following condition holds

$$(2c - a^2 + b^2) > 0, \text{ and } (c^2 - d^2) > 0.$$

When either condition is satisfied, the system transits from the locally stable regime to instability as  $\tau_1$  increases beyond a critical value. However, when condition 2 is satisfied, further increase in delay could lead to restabilisation of the system. This implies that the system could undergo stability switches when condition 2 is satisfied [4]. Since extensive simulations suggest the nonoccurrence of stability switches in the system, we focus only on the case when condition 1 is satisfied and only one positive value of  $\omega^2$  exists. This implies that there exists a cross over frequency at which one pair of complex conjugate roots crosses over the imaginary axis and the system transits from a locally stable to an unstable regime. The critical value of  $\tau_1$ , denoted by  $\tau_{1,c}$ , at which this transition occurs is given by

$$\tau_{1,c} = \frac{1}{\omega} \cos^{-1} \left( \frac{\omega^2(d-ab)-cd}{b^2\omega^2+d} \right).$$

It can be analytically shown that this loss of stability occurs via a Hopf bifurcation when one pair of complex conjugate roots of (32) crosses over the imaginary axis with non-zero velocity at  $\tau_1 = \tau_{1,c}$ . Hence, we can conclude that the necessary and sufficient condition for the system (41) to be locally stable about its equilibrium is

$$\tau_1 < \frac{1}{\omega} \cos^{-1} \left( \frac{\omega^2(d - ab) - cd}{b^2\omega^2 + d} \right).$$

■

This condition essentially captures the interdependence among different network parameters and Compound TCP parameters to ensure stability of the system.

### B. Hopf Condition

We have seen that an increase in delay above the critical delay value prompts the system to transit from stability to instability. Varying any of the system parameters beyond the critical value can also drive the system to instability. Thus, instead of treating delay or any of the system parameters as the bifurcation parameter, we introduce an exogenous non-dimensional parameter  $\kappa$  which can act as the bifurcation parameter. If  $\kappa$  is varied keeping the values of the system parameters constant at their critical values, the system loses stability at  $\kappa_c = 1$ . To show that this loss of stability occurs via a Hopf bifurcation, we proceed to verify the transversality condition of the Hopf spectrum [11, Chapter 11, Theorem 1.1. ] for both scenarios. To verify the transversality condition, we need to show that  $\text{Re}(d\lambda/d\kappa) \neq 0$  at  $\kappa = \kappa_c$ .

#### Case I

In this scenario, the linearised system, with the non-dimensional parameter  $\kappa$ , becomes

$$\begin{aligned} \dot{u}_1(t) &= \kappa \left( -au_1(t) - bu_1(t - \tau) - cu_2(t - \tau) \right), \\ \dot{u}_2(t) &= \kappa \left( -au_2(t) - bu_2(t - \tau) - cu_1(t - \tau) \right). \end{aligned} \quad (45)$$

Looking for exponential solutions of (45) we get

$$(\lambda + \kappa a + \kappa(b + c)e^{-\lambda\tau})(\lambda + \kappa a + \kappa(b - c)e^{-\lambda\tau}) = 0. \quad (46)$$

Differentiating (46) with respect to  $\kappa$ , we get

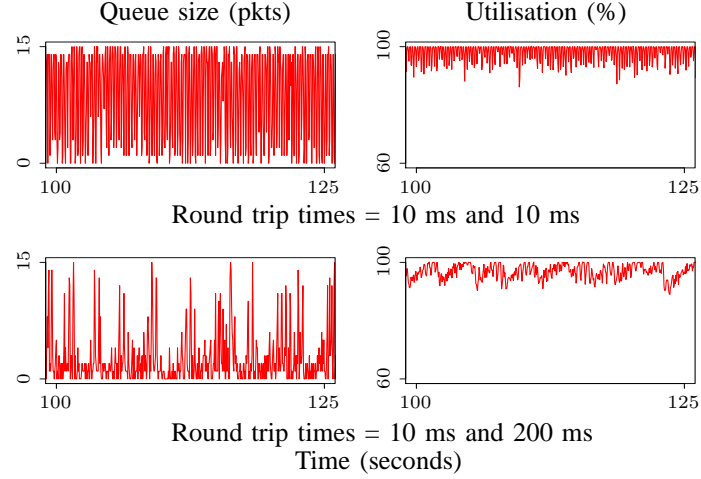
$$\frac{d\lambda}{d\kappa} = \frac{-\kappa a^2 - \lambda a - \lambda b e^{-\lambda\tau} - 2\kappa a b e^{-\lambda\tau} - \kappa(b^2 - c^2)e^{-2\lambda\tau}}{\lambda + \kappa a + \kappa b e^{-\lambda\tau} - \lambda \kappa b \tau e^{-\lambda\tau} - \kappa^2 a b \tau e^{-\lambda\tau} - \kappa^2 \tau(b^2 - c^2)e^{-2\lambda\tau}}. \quad (47)$$

From (46) we get,

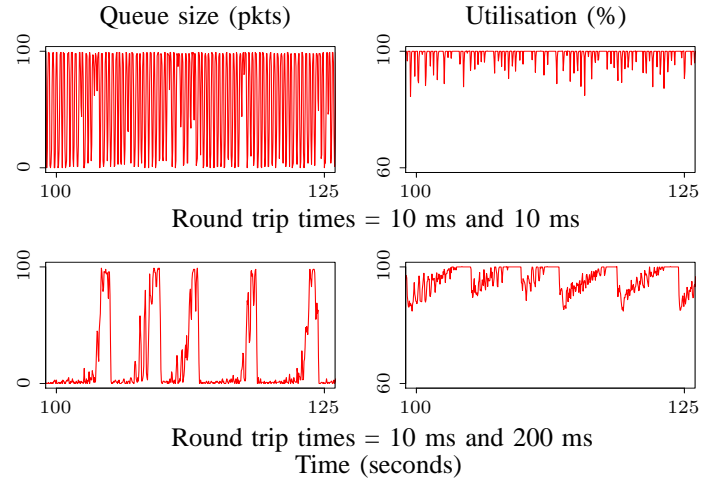
$$e^{-\lambda\tau} = -\frac{\lambda + \kappa a}{\kappa(b + c)}. \quad (48)$$

Next, substituting (48) in (47), we get

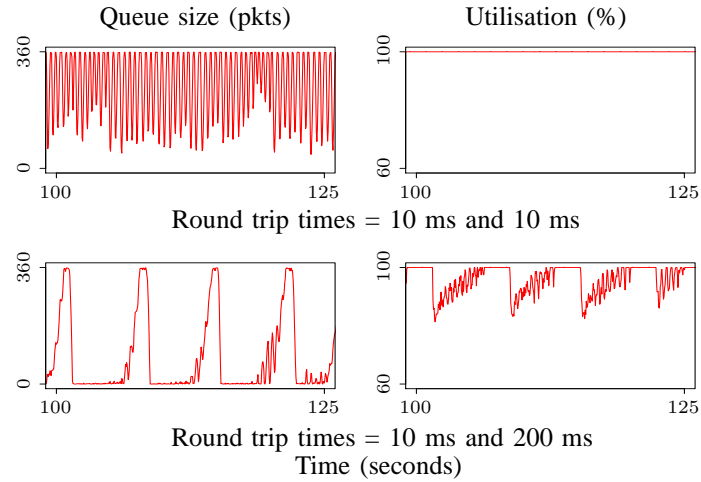
$$\frac{d\lambda}{d\kappa} = \frac{\lambda}{\kappa(1 + \lambda\tau + \kappa a\tau)}. \quad (49)$$



(a) Buffer size = 15

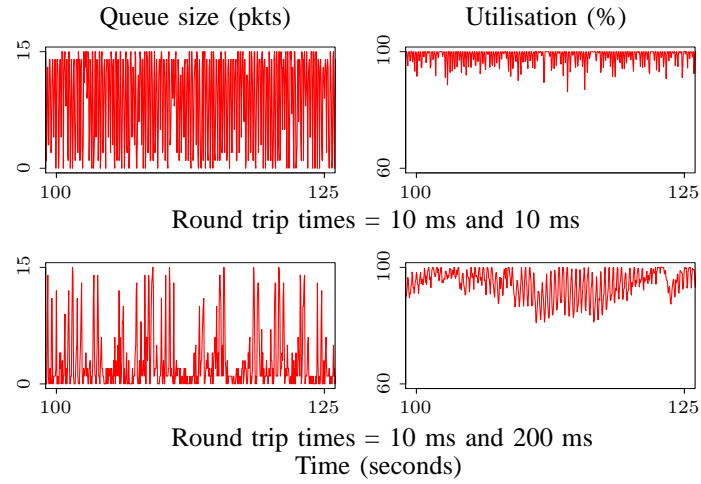


(b) Buffer size = 100

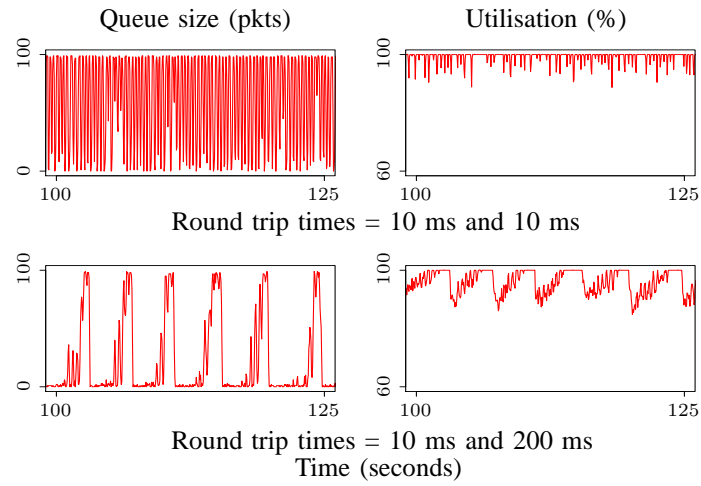


(c) Buffer size = 360

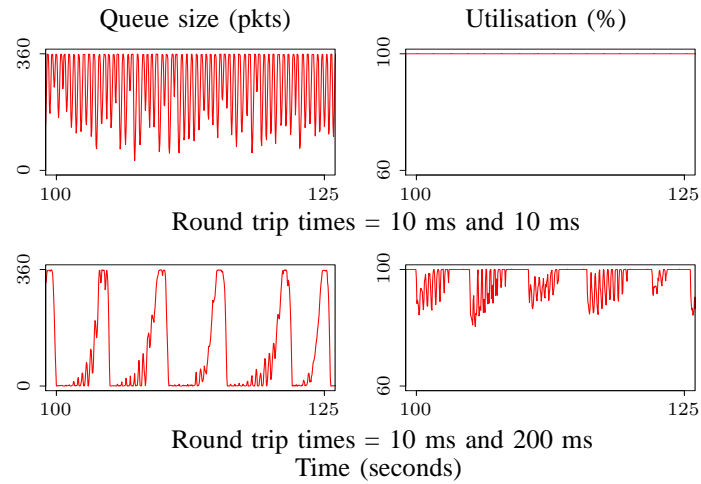
Fig. 8: *Long-lived flows*. Two sets of 60 long-lived Compound flows over a 2 Mbps link, regulated by two edge routers, feeding into a core router with link capacity 180 Mbps.



(a) Buffer size = 15



(b) Buffer size = 100



(c) Buffer size = 360

Fig. 9: *Long-lived and short-lived flows.* Two sets of 60 long-lived Compound flows over a 2 Mbps link, along with *exponentially distributed short files*, regulated by two edge routers and feeding into a core router with capacity 180

Mbps.

August 22, 2018

DRAFT

At  $\tau = \tau_0$ ,  $\kappa = \kappa_c$ . Substituting  $\lambda = j\omega_1$  in (49) we get

$$\operatorname{Re} \left( \frac{d\lambda}{d\kappa} \right)_{\lambda=j\omega_1} = \frac{\omega_1^2 \tau_0}{\kappa_c \left( (1 + \kappa_c a \tau_0)^2 + (\omega_1 \tau_0)^2 \right)} > 0.$$

In particular, we have proved that,  $\operatorname{Re}(d\lambda/d\kappa) > 0$ , which implies that the roots cross over the imaginary axis with positive velocity at  $\kappa = \kappa_c$ .

### Case II

For the second scenario, we observe that the linearised system, with the non-dimensional exogenous parameter  $\kappa$  is given as

$$\begin{aligned} \dot{u}_1(t) &= \kappa \left( \mathcal{M}_1 u_1(t) - \mathcal{N}_1 u_1(t - \tau_1) - \mathcal{P}_1 u_2(t - \tau_2) \right), \\ \dot{u}_2(t) &= \kappa \left( -(\mathcal{M}_2 + \mathcal{N}_2) u_2(t) - \mathcal{P}_2 u_1(t - \tau_1) \right). \end{aligned} \quad (50)$$

To show that system (50) loses stability via a Hopf bifurcation as the non-dimensional parameter  $\kappa$  is increased, we need to verify the transversality of the Hopf spectrum. Note that, for any complex number  $z$ ,  $\operatorname{Re}(z) \neq 0$  if and only if  $\operatorname{Re}(z^{-1}) \neq 0$ . Hence, for ease of analysis, we proceed to verify that  $\operatorname{Re}(d\lambda/d\kappa) \neq 0$  at  $\kappa = \kappa_c$ . Looking for exponential solution of (50) leads us to the following characteristic equation:

$$\lambda^2 + \kappa a \lambda + \kappa b \lambda e^{-\lambda \tau_1} + \kappa^2 c e^{-\lambda \tau_1} + \kappa^2 d = 0. \quad (51)$$

Differentiating (51) with respect to  $\kappa$ , we get

$$\frac{d\lambda}{d\kappa} = \frac{-a\lambda - b\lambda e^{-\lambda \tau_1} - 2\kappa c e^{-\lambda \tau_1} - 2\kappa d}{2\lambda + \kappa a + \kappa b e^{-\lambda \tau_1} - \kappa b \lambda \tau_1 e^{-\lambda \tau_1} - \kappa^2 c \tau_1 e^{-\lambda \tau_1}} \quad (52)$$

From the characteristic equation (51), we get

$$e^{-\lambda \tau_1} = -\frac{\lambda^2 + \kappa a \lambda + \kappa^2 d}{\kappa b \lambda + \kappa^2 c}. \quad (53)$$

Now, substituting the value of  $e^{-\lambda \tau_1}$  in (52) and performing some algebraic manipulations, we obtain

$$\left( \frac{d\lambda}{d\kappa} \right)^{-1} = \left( \frac{d\lambda}{d\kappa} \right)_1^{-1} + \left( \frac{d\lambda}{d\kappa} \right)_2^{-1} + \left( \frac{d\lambda}{d\kappa} \right)_3^{-1},$$

where,

$$\begin{aligned} \left( \frac{d\lambda}{d\kappa} \right)_1^{-1} &= \frac{\kappa}{\lambda}, \quad \left( \frac{d\lambda}{d\kappa} \right)_2^{-1} = \kappa \tau_1, \\ \left( \frac{d\lambda}{d\kappa} \right)_3^{-1} &= \frac{\kappa^2 (\lambda^2 a b \tau_1 - \lambda^2 c \tau_1 + 2\kappa \lambda b d \tau_1 + \kappa^2 c d \tau_1)}{\lambda (\lambda^2 b + \kappa^2 a c + 2\kappa \lambda c - \kappa^2 b d)}. \end{aligned} \quad (54)$$

Recall that, at the crossover point, the system has one pair of complex conjugate roots on the imaginary axis. Hence, substituting  $\lambda = j\omega$  in (54), we obtain  $\left( \frac{d\lambda}{d\kappa} \right)_{1,\lambda=j\omega}^{-1} = \frac{\kappa}{j\omega}$ , which is purely imaginary. Similarly, we see that

$\left(\frac{d\lambda}{d\kappa}\right)_{2,\lambda=j\omega}^{-1} = \kappa\tau_1$  which is strictly positive. Thus, to verify that  $\text{Re}\left(\frac{d\lambda}{d\kappa}\right)_{\lambda=j\omega}^{-1} > 0$ , verifying  $\text{Re}\left(\frac{d\lambda}{d\kappa}\right)_{3,\lambda=j\omega}^{-1} > 0$  suffices. Now,

$$\text{Re}\left(\frac{d\lambda}{d\kappa}\right)_{3,\lambda=j\omega}^{-1} = \frac{2\omega^2\kappa^3\tau_1(abc - c^2 - bd^2)(\omega^2 + \kappa^2d)}{4\omega^4\kappa^2c + (\kappa^2\omega ac - \omega^3b - \kappa^2\omega bd)^2}. \quad (55)$$

Recall that  $d$  is positive. Hence, the expression  $\omega^2 + \kappa^2d$  is positive. Thus, it suffices to verify that  $(abc - c^2 - bd^2) > 0$ . Substituting the values of  $a, d, c$  and  $d$  from (44), we get

$$\begin{aligned} abc - c^2 - bd^2 &= 2N_1N_2P_1P_2 - P_1^2P_2^2 - N_1M_1P_1P_2 \\ &= P_1P_2(N_1N_2 - P_1P_2) + N_1P_1P_2(N_2 - M_1). \end{aligned}$$

Recall that,  $M_j, N_j$  and  $P_j$  are strictly positive for  $j = 1, 2$ . Now, it can be easily concluded that  $N_1N_2 > P_1P_2$ . Hence, the first term in the above expression is positive. Further, we note that, with the assumption  $\tau_1 \gg \tau_2$  and  $\tau_2 \approx 0$ ,  $N_2$  becomes unbounded but  $M_1$  remains bounded. Thus, we can assume that, in this regime,  $N_2 \gg M_1$  which ensures that  $abc - c^2 - bd^2 > 0$ . Hence, we can conclude that  $\text{Re}\left(\frac{d\lambda}{d\kappa}\right)_{3,\lambda=j\omega}^{-1} > 0$ , which in turn ensures that

$$\text{Re}\left(\frac{d\lambda}{d\kappa}\right)_{\lambda=j\omega}^{-1} > 0.$$

Thus, we observe that, the system undergoes a *Hopf Bifurcation* at  $\kappa = \kappa_c$  for both scenarios. This implies that the system loses stability, as the system parameters vary, leading to the emergence of limit cycles in the system dynamics. These limit cycles could in turn induce synchronisation among the Compound TCP flows which leads to periodic packet losses and makes the downstream traffic bursty.

### C. Simulations

To validate our analytical insights, we simulate two scenarios in the multiple bottleneck topology: only long-lived flows, and a combination of long and short flows.

The system consists of two distinct sets of 60 Compound TCP flows, regulated by two edge routers, feeding into a common core router. The round trip time of one set of TCP flows is fixed at 10 ms, and that of the other set of flows is varied from 10 ms to 200 ms. The short-lived flows are exponentially distributed with a mean file size of 1Mb. Each edge router has a link capacity of 100 Mbps and the core router has a link capacity of 180 Mbps. In the small buffer regime, we fix the edge router buffers to 15 packets and the core router buffer size is varied from 15 packets to 100 packets. We recapitulate that in the intermediate buffer regime, the proposed buffer dimensioning rule is  $C \cdot RTT/\sqrt{N}$ . Using this buffer dimensioning rule, we fix the edge router buffers to be 270 packets and the core router buffer to be 360 packets.

Fig. 8 shows the simulations when there are only long-lived flows in the system. It is clear that larger queue threshold leads to non-linear oscillations, in the form of limit cycles, in the queue size. Such limit cycles can have a detrimental effect on link utilisation. Fig. 9 shows the simulations when there is a combination of long and short flows. Clearly, the time-delayed feedback effects of the long flows dominates the system stability and dynamics.



## V. CONCLUDING REMARKS

In this paper, we conducted a performance evaluation of Compound TCP in two different topologies, with Drop-Tail queues, under two buffer sizing regimes: an intermediate and a small buffer regime. For the traffic, we considered either just long-lived flows, or a combination of long and short flows. Using a combination of analysis and packet-level simulations, we explored numerous dynamical and some statistical properties to obtain a few key insights.

From a dynamical perspective, we emphasised the interplay between buffer sizes and stability. In particular, we showed that larger queue thresholds may help link utilisation, but they would increase queuing delay and are also prone to inducing limit cycles, via a Hopf bifurcation, in the queue size dynamics. However, such limit cycles can in turn lead to a drop in link utilisation, induce synchronisation among TCP flows, and make the downstream traffic bursty.

We also noted that when a network has a combination of long and short flows, then despite the presence of short flows, such limit cycles continue to exist in the queue size. Some design considerations for protocol and network parameters, to ensure stability and low-latency queues, are also outlined. We repeatedly witnessed the existence of limit cycles in the queue size. To that end, it would be of both theoretical and practical interest, to establish the *asymptotic orbital stability* of the bifurcating limit cycles and to determine the *type* of the Hopf bifurcation. One way to approach this analytically would be via the theory of normal forms and the centre manifold analysis [9], and such an analysis is conducted in a sequel to this work.

In terms of the statistical properties, we examined the empirical queue distribution for the core router, in a single bottleneck topology. We observed that in a high bandwidth-delay product and a small buffer regime, and with a large number of long-lived flows, the bottleneck queue may be approximated by an  $M/M/1/B$  or an  $M/D/1/B$  queue. This makes the system model amenable to analysis, and thus gives confidence in using the underlying model to better understand network performance and quality of service.

Our work opens numerous avenues that merit further investigation. We certainly need a better understanding of the statistical properties of the queues, specially in multiple bottleneck topologies. It would also be useful to explore network performance when we move away from the assumption of long-lived flows. Moving to a small buffer regime is a potentially long-term solution. In the interim, one needs to explore the design of queue management strategies that are able to ensure both low-latency and stable queue sizes.

## REFERENCES

- [1] L.S. Brakmo and L.L. Peterson, “TCP Vegas: end to end congestion avoidance on a global Internet”, *IEEE Journal on Selected Areas in Communications*, vol. 13, pp. 1465–1480, 1995.
- [2] S.A. Campbell, S. Ruan and J. Wei, “Qualitative analysis of a neural network model with multiple time delays”, *International Journal of Bifurcation and Chaos*, vol. 9, pp. 1585–1595, 1999.
- [3] V.G. Cerf, “Bufferbloat and other Internet challenges”, *IEEE Internet Computing*, vol. 5, pp. 79–80, 2014.
- [4] K.L. Cooke, and Z. Grossman, “Discrete delay, distributed delay and stability switches”, *Journal of Mathematical Analysis and Applications*, vol. 86, pp. 592–627, 1982.

- [5] S. Floyd and V. Jacobson, "Random Early Detection gateways for congestion avoidance", *IEEE/ACM Transactions on Networking*, vol. 1, pp. 397–413, 1993.
- [6] S. Floyd, "HighSpeed TCP for large congestion windows", RFC 3649, December 2003.
- [7] J. Gettys and K. Nichols, "Bufferbloat: dark buffers in the Internet", *Communications of the ACM*, vol. 55, pp. 57–65, 2012.
- [8] D. Ghosh, K. Jagannathan, and G. Raina, "Right buffer sizing matters: stability, queuing delay and traffic burstiness in compound TCP", in *Proceedings of 52nd Annual Allerton Conference on Communication, Control, and Computing*, 2014.
- [9] J. Guckenheimer and P. Holmes, *Nonlinear Oscillations, Dynamical Systems, and Bifurcations of Vector Fields*, Springer-Verlag, 1996.
- [10] S. Ha, I. Rhee and L. Xu, "CUBIC: a new TCP-friendly high-speed TCP variant", *ACM SIGOPS Operating Systems Review*, vol. 42, pp. 64–74, 2008.
- [11] J.K. Hale and S.M.V. Lunel, *Introduction to functional differential equations*, Springer Science & Business Media, 2013.
- [12] J.K. Hale, L.T. Magalhães, and W. Oliva, *Dynamics in infinite dimensions*, Springer Science & Business Media, 2006.
- [13] H. Jiang, Y. Wang, K. Lee, and I. Rhee, "DRWA: a receiver-centric Solution to Bufferbloat in Cellular Networks", to appear in *IEEE Transactions on Mobile Computing*.
- [14] F.P. Kelly, "Models for a self-managed Internet", *Philosophical Transactions of the Royal Society of London A: Mathematical, Physical and Engineering Sciences*, vol. 358, pp. 2335–2348, 2000.
- [15] K. Nichols and V. Jacobson, "Controlling queue delay", *Communications of the ACM*, vol. 55, pp. 42–50, 2012.
- [16] J. Padhye, V. Firoiu, D. Towsley and J.F. Kurose, "Modeling TCP Reno performance: a simple model and its empirical validation", *IEEE/ACM Transactions on Networking*, vol. 8, pp. 133–145, 2000.
- [17] R. Pan, P. Natarajan, C. Piglione, M.S. Prabhu, V. Subramanian, F. Baker, and B. VerSteeg, "PIE: a lightweight control scheme to address the bufferbloat problem", in *Proceedings of 14th International Conference on High Performance Switching and Routing (HPSR)*, 2013.
- [18] G. Raina, "Local bifurcation analysis of some dual congestion control algorithms", *IEEE Transactions on Automatic Control*, vol. 50, pp. 1135–1146, 2005.
- [19] G. Raina, S. Manjunath, S. Prasad, and K. Giridhar, "Stability and performance analysis of Compound TCP With REM and Drop-Tail queue management", to appear in *IEEE/ACM Transactions on Networking*.
- [20] G. Raina and D. Wischik, "Buffer sizes for large multiplexers: TCP queueing theory and instability analysis", in *Proceedings of Next Generation Internet Networks*, 2005.
- [21] P. Raja and G. Raina, "Delay and loss-based transport protocols: buffer-sizing and stability", in *Proceedings of International Conference on Communication Systems and Networks*, 2012.
- [22] A. Showail, K. Jamshaid, and B. Shihada, "Buffer sizing in wireless networks: challenges, solutions, and opportunities", *IEEE Communications Magazine*, 2014.
- [23] S. Sojoudi, S.H. Low and J.C. Doyle, "Buffering dynamics and stability of Internet congestion controllers", *IEEE/ACM Transactions on Networking*, vol. 22, pp. 1808–1818, 2014.
- [24] K. Tan, J. Song, Q. Zhang and M. Sridharan, "A Compound TCP approach for high-speed and long distance networks", in *Proceedings of IEEE INFOCOM*, 2006.
- [25] D. Wischik and N. McKeown, "Part I: Buffer sizes for core routers", *ACM Computer Communication Review*, vol. 35, pp. 75–78, 2005.
- [26] P. Yang, J. Shao, W. Luo, L. Xu, J. Deogun, and Y. Lu, "TCP congestion avoidance algorithm identification", *IEEE/ACM Transactions on Networking*, vol. 22, pp. 1311–1324, 2014.
- [27] P. Yang, E. Zhang, and L. Xu, "Sizing router buffer for the Internet with heterogeneous TCP", in *Proceedings of 32nd International Performance Computing and Communications Conference (IPCCC)*, 2013.
- [28] The Network Simulator (NS2). [Online]. Available: [http://nsnam.isi.edu/nsnam/index.php/User Information](http://nsnam.isi.edu/nsnam/index.php/User%20Information).

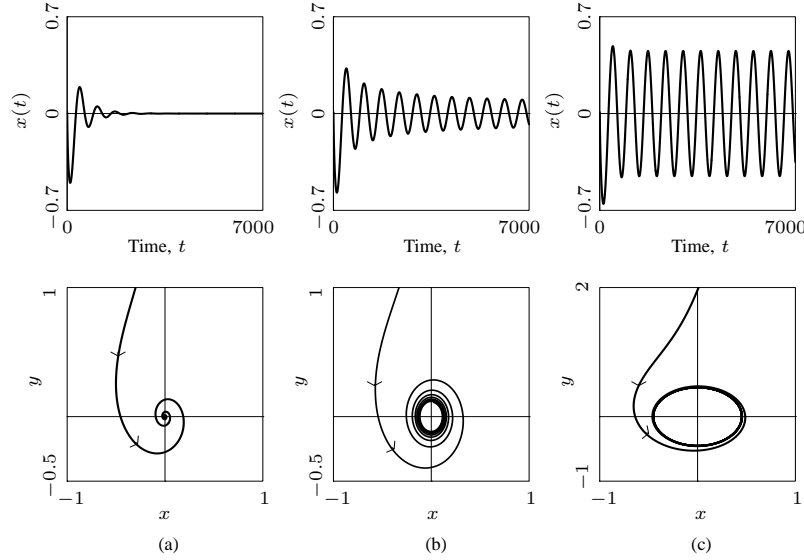


Fig. 10: *Solutions and phase portraits for a supercritical Hopf bifurcation.* (a)  $\alpha < 0$ , (b)  $\alpha = 0$  and (c)  $\alpha > 0$ . Note that, the first row corresponds to the time-domain solutions whereas the second row corresponds to the phase portraits.

## APPENDIX I

In this Appendix, we provide a brief description of the Hopf bifurcation phenomenon in dynamical systems. Consider the following system of ordinary differential equations (ODE)

$$\dot{x} = f(x, \alpha), \quad x \in \mathbb{R}^n. \quad (56)$$

Here, let  $f$  be a smooth function. Notice that (56) is parametrised by  $\alpha \in \mathbb{R}$ . Without loss of generality, we assume that  $x = 0$  is an equilibrium for system (56) for all sufficiently small  $|\alpha|$ . Further, we assume that at  $\alpha = 0$ , the system has one pair of purely imaginary roots  $\lambda = \pm i\omega_0$ ,  $\omega_0 > 0$ . Thus, as  $\alpha$  is varied in a small neighbourhood of zero, the equilibrium changes its stability as one pair of complex conjugate roots crosses over the imaginary axis. This leads to the appearance or disappearance of an isolated periodic orbit, termed as a *limit cycle*. At  $\alpha = 0$ , the system is said to undergo a *Hopf bifurcation*, which can be of two types: *supercritical* and *subcritical*.

To determine if a given parametrised system of ODEs undergo a Hopf bifurcation, we first linearise the system about the desired equilibrium. We then derive the *characteristic equation* of this system by looking for exponential solutions. We then search for a value of the parameter where a conjugate pair of purely imaginary eigenvalues exists. Finally, we prove the *transversality of the Hopf spectrum*, *i.e.*, we show that the eigenvalues cross over into the right half of the Argand plane, as the parameter is varied about the critical value. This in turn leads to the appearance or disappearance of limit cycles in system dynamics.

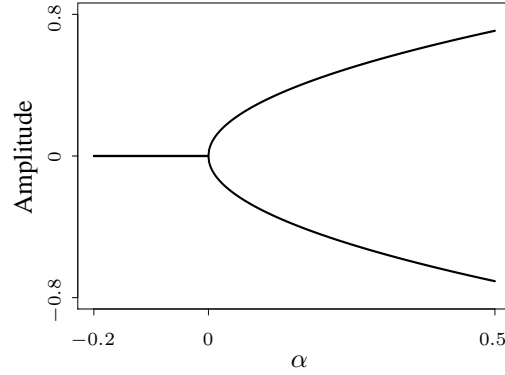


Fig. 11: *Bifurcation diagram for a supercritical Hopf bifurcation* showing the variation in the amplitude of the emergent limit cycle in the dynamics of the state variable  $x(t)$ , as  $\alpha$  is just increased beyond zero.

We now briefly explain the supercritical Hopf bifurcation through an example. Consider the following system of ODEs:

$$\begin{aligned}\dot{x} &= \alpha x - y - x(x^2 + y^2), \\ \dot{y} &= x + \alpha y - y(x^2 + y^2).\end{aligned}\tag{57}$$

Note that the above system of differential equations is parametrised by  $\alpha$ . For all values of  $\alpha$ ,  $x^* = y^* = 0$  is an equilibrium for system (57). We then linearise the system about this equilibrium. When  $\alpha < 0$ , the equilibrium is linearly stable. At  $\alpha = 0$ , the equilibrium is marginally stable, and the system undergoes a Hopf bifurcation at this point. For  $\alpha > 0$ , the equilibrium loses its stability and an orbitally stable limit cycle with radius  $\sqrt{\alpha}$  emerges, thus making the equilibrium an unstable focus. This change in the topological behaviour of the system with a variation in  $\alpha$ , is illustrated in Fig. 10. Fig. 11 shows the variation in the amplitude of the emergent limit cycle in the state variable  $x(t)$ , when the system is pushed beyond the edge of stability by a sufficiently small increase in  $\alpha$ . It would be worthwhile to mention that the dynamics of the state variable  $y(t)$  exhibit similar qualitative changes with variation in the parameter  $\alpha$ .

Note that, the models which we consider in this paper are non-linear, time-delayed differential equations, which are infinite-dimensional systems. Analysing the bifurcation properties of such systems is rather difficult; for a detailed discussion, see [11] and [12]. While the topological features are similar for the case of delayed systems, the algebraic manipulations are cumbersome. To that end, this discussion on ODEs provides a basic understanding of Hopf bifurcation.